Am J Transl Res 2017;9(12):5743-5753
www.ajtr.org /ISSN:1943-8141/AJTR0058002

Original Article

MiR-30a attenuates osteoclastogenesis via targeting DC-STAMP-c-Fos-NFATc1 signaling

Yiran Yin[1], Lian Tang[1], Jieying Chen[2], Xiaobo Lu[1]

[1]*The Orthopaedic Department, The Affiliated Hospital of Southwest Medical University, Luzhou City, Sichuan Province, China;* [2]*The Department of Burns and Plastics Surgery, The Affliated Hospital of Southwest Medical University, Luzhou City, Sichuan Province, China*

Received May 22, 2017; Accepted October 15, 2017; Epub December 15, 2017; Published December 30, 2017

Abstract: Osteoclast is a kind of unique cells which is responsible for bone matrix absorption. It was widely reported that microRNAs (miRNAs) could regulate several physiological processes, including osteoclastogenesis. In our study, microarray analysis showed that miR-30a was down-regulated during osteoclastogenesis after RANKL (receptor activator of nuclear factor κB ligand) stimulation. Osteoclasts and actin-ring formation as well as bone resorption were inhibited when miR-30a was overexpressed in osteoclast precursor cells. Meantime, when miR-30a was inhibited in osteoclast precursor cells, osteoclasts and actin-ring formation as well as bone resorption were promoted. Furthermore, we discovered that miR-30a overexpression inhibited the protein levels of DC-STAMP, c-Fos and NFATc1. However, when DC-STAMP was inhibited by using a DC-STAMP siRNA, we could not detect the inhibition effect of osteoclastogenesis and bone resorption induced by miR-30a. In conclusion, miR-30a attenuated osteoclastogenesis via suppression of DC-STAMP-c-Fos-NFATc1 signaling pathway. On these grounds, this study may reveal a new promising target for the treatment of osteoporosis and other osteopenic disorders.

Keywords: DC-STAMP, osteoclastogenesis, microRNA, c-Fos, NFATc1

Introduction

Bone remodeling is a constant process to maintain skeletal integrity and strength. During this process, osteoclasts have the responsibility for resorbing old bone, while osteoblasts play key role in forming new bone. According to numerous reports, the imbalance during bone remodeling caused by either osteoclasts or osteoblasts could cause various kinds of osteopenic diseases including osteoporosis [1, 2].

Osteoclasts, derived from hematopoietic stem cells, are a kind of multinucleated giant cells, which function as bone resorption cells [3]. The most important step during the formation of multinucleated mature osteoclasts from hematopoietic precursors is osteoclast precursor (OCP) fusion [4]. As numerous researches have suggested that by replacing old bone with new one, osteoclasts take part in maintaining bone homeostasis [5, 6], deep insight of the related mechanisms involved in osteoclastogenesis and bone resorption is of significant importance for the management of osteopenic disorders.

MicroRNAs (miRNAs), a kind of endogenous small, noncoding RNA, include 18 to 22 nucleotides [7]. It can inhibit gene expression post-transcriptionally through binding with complementary sequences of protein coding transcripts which are mainly in the 3'-UTRs. Protein synthesis can be selectively suppressed as a result of the binding of a miRNA to the target sequences of protein [8, 9]. MicroRNAs have been reported to regulate a lot of genes, thus affecting various kinds of cell activities and maintaining homoeostasis [7]. Numerous evidence has proved that abnormal expression of miRNAs can contribute to bone degeneration-related diseases, via regulating the formation of osteoclasts as well as bone resorption [10-12].

In this study, miRNA array revealed that miR-30a was down-regulated in the process of osteoclastogenesis. Through deep investigating the underlying mechanism involved, we con-

cluded that DC-STAMP-c-Fos-NFATc1 pathway was a target of miR-30a in regulating osteoclastogenesis and bone absorption.

Materials and methods

Osteoclast formation and TRAP staining

We isolated murine osteoclasts from bone marrow which were mentioned previously [13]. Briefly speaking, we isolated bone marrow cells and then cultured them in α-MEM (Sigma) supplemented with 10% FBS (GIBCO). After incubating bone marrow cells with M-CSF (20 ng/ml) (R&D Systems Inc) for 48 hours, we considered adherent cells as bone marrow-derived monocytes (BMMs). Then we cultured BMMs with 30 ng/ml M-CSF and 100 ng/ml RANKL for 4 days to generate osteoclasts. Osteoclasts induced in the culture were assessed by TRAP staining. TRAP + multinuclear osteoclasts (>3 nuclei) appeared as dark purple cells and were counted by light microscopy.

MiRNA microarray analysis

M-CSF (30 ng/ml) supplemented with 100 ng/ml RANKL were used to culture BMMs for the indicated times. Total RNAs of each sample were isolated following the instructions. We purchased the mouse miRNA Expression Profiling array V.2 from the company of Illumina Inc. and the expression levels were determined. A total of 656 assays were included in our assay panel for mouse miRNAs which were described in the miRBase database v9.1. Following the instructions from the manufacturer, we performed RT-PCR with miRNAs. The array data was extracted with BeadStudio v3.1.3 (Illumina). After being log transformed and normalized, the values were determined similarity by Hierarchical clustering. At last, we selected miRNAs in experiment groups that have at least two times difference compared with control groups regarding expression level to make the expression profile.

Actin ring staining

Both 30 ng/ml M-CSF and 100 ng/ml RANKL were used to culture BMMs to generate osteoclast precursors (OCPs). 30 ng/ml M-CSF and 50 ng/ml RANKL were used to culture OCPs for another 24 h. Cells were incubated with PBS supplemented with 0.1% Triton X-100 for 5 min after fixation and immunostained with Alexa Fluor 488-phalloidin (Molecular Probes).

Pit formation assay

Firstly, we plated BMMs on Osteo Assay plates (Corning) and cultured them with M-CSF and RANKL for 48 hours to generate OCPs. M-CSF of 30 ng/ml supplemented with RANKL of 50 ng/ml were used to culture OCPs for another 36 hours. OD values were determined according to the amount of pits.

Transfection

MiR-30a mimic, inhibitor, and a negative control (NC) with fluorescent tags were synthesized by Shanghai GenePharma (China). OCPs were transfected with miR-30 mimics, inhibitors and negative control, respectively. 4-6 hours post-transfection, cell culture media was changed. Then M-CSF and RANKL were used to culture transfected cells for another 24-36 hours. We purchased Gene-specific siRNAs as well as non-targeting siRNA from Shanghai GenePharma (China). The sequence of DC-STAMP siRNA was 5'-GCTGGAAGTTCACTTGAAACT-3' and the sequence of the non-targeting control siRNA was 5'-UUCUCCGAACGUGUCACGUTT-3'. The transfection of small interfering RNAs into cells were done according to above protocols.

RT-qPCR

To determine the relative expression levels of RNA during osteoclastogenesis, cells were lysed with TRIzol regent and extracted RNA. After whole RNA extraction, a PrimeScript RT kit purchased from TaKaRa was used to reverse transcription. The reversed cDNA were ready for qRT-PCR. These following primers were used: U6 (forward: 5'-AGA GAA GAT TAG CAT GGC CCC TG-3', reverse: 5'-ATC CAG TGC AGG GTC CGA GG-3'); NFATc1 (forward: 5'-AAG AGG AAG TAC AGC CTC AAC G-3', reverse: 5'-TCT CCT TTC CGA AGT TCA ATG T-3'); β-actin (forward: 5'-TCC TGT GGC ATC CAC GAA ACT-3', reverse: 5'-GAA GCA TTT GCG GTG GAC GAT-3'). U6 and β-actin were used as internal reference. The $2^{-\Delta\Delta Ct}$ equation was used to determine the relative expression levels.

Luciferase reporter assay

The luciferase reporter vector of DC-STAMP 3'-UTR was ordered from Shanghai Genechem (China). Stratagene QuikChange Lightning Site-directed Mutagenesis Kit (Agilent Technologies) was used to perform site directed mutagenesis by using. To detect repression by miR-30a,

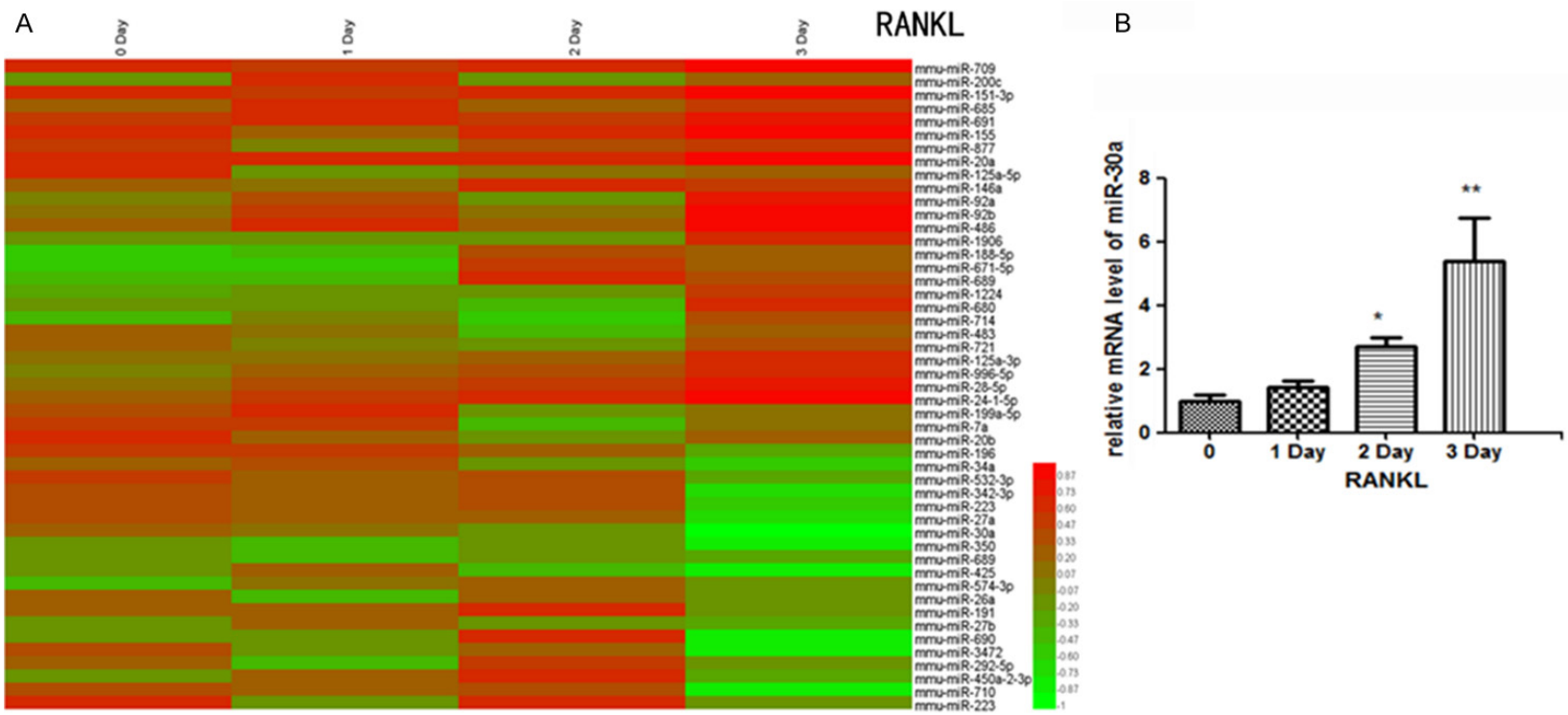

Figure 1. miR-30a is down-regulated during RANKL induced osteoclastogenesis. (A) Microarray analysis was performed using RNAs isolated during RANKL induced osteoclast differentiation. High expression levels of miRNAs are indicated in red, whereas low expression levels of miRNAs are depicted in green. (B) Validation of microarray data by qRT-PCR analysis of miR-30a expression. The PCR products were normalized to U6 level for each reaction. Data represent means ± SD of triplicate samples. Results are representative of at least three independent sets of similar experiments. *$p < 0.05$, **$p < 0.01$ vs. control BMMs.

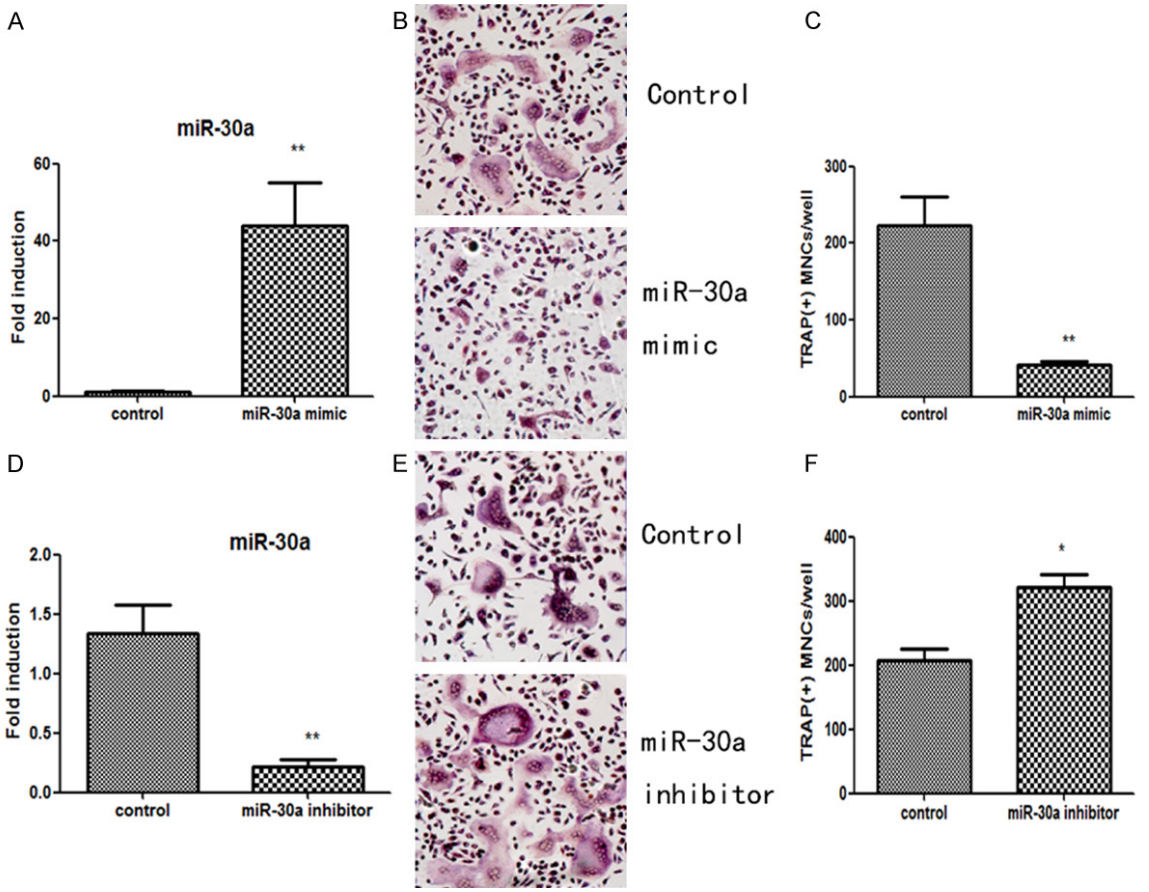

Figure 2. miR-30a inhibits RANKL-induced osteoclast formation. BMMs were cultured for 2 days in the presence of MCSF and RANKL. (A, C) Two-day-old OCPs were transfected with the miR-30a mimic or a negative control. (A) Expression level of miR-30a was detected by qRT-PCR. Data represent means ± SD of triplicate samples. **p < 0.001 vs. control. (B, C) Transfected OCPs were cultured for an additional 24 h with M-CSF and RANKL. (B) Cultured cells were fixed and stained for TRAP. (C) Numbers of TRAP + MNCs were counted. Data represent means ± SD of triplicate samples. **p < 0.001 vs. control. Results are representative of at least three independent sets of similar experiments. (D, E) OCPs were transfected with miR-30a inhibitor or negative control. (D) Expression level of miR-30a was detected by qRT-PCR. Data represent means ± SD of triplicate samples. **p < 0.001 vs. control. (E, F) Transfected OCPs were cultured for an additional 24 h with M-CSF and RANKL. (E) Cultured cells were fixed and stained for TRAP. (F) Numbers of TRAP + MNCs were counted. Data represent means ± SD of triplicate samples. *p < 0.05 vs. control. Results are representative of at least three independent sets of similar experiments.

HEK293T cells were cotransfected with the indicated DC-STAMP 3'-UTR luciferase reporter (with either wild-type or mutant-type miR-30a binding sites). The Renilla luciferase was transfected as an efficiency control. The luciferase activity was measured using luciferase assay system (Promega) according to the instructions of the manufacturers.

Western blot analysis

After washing with ice-cold PBS, cells were lysed with PIPA buffer (Beyotime) to get total protein. We determined protein concentration with a protein assay kit. 10% SDS-PAGE was used to separate protein. And then it was shifted to PVDF membranes purchased from Millipore. 5% fat-free milk was used to block non-specific protein interactions in TBST buffer. The membranes loaded with proteins were incubated at 4°C with primary antibody and incubated at room temperature with secondary antibody conjugated with horseradish peroxide (two hours). After washing these membranes in TBST buffer, we developed the membranes using chemiluminescence to detect antibodies concentration and took GAPDH as our internal control. The antibodies, anti-DC-STAMP, anti-c-Fos, anti-NFATc1 and anti-GAPDH were purchased from Abcam.

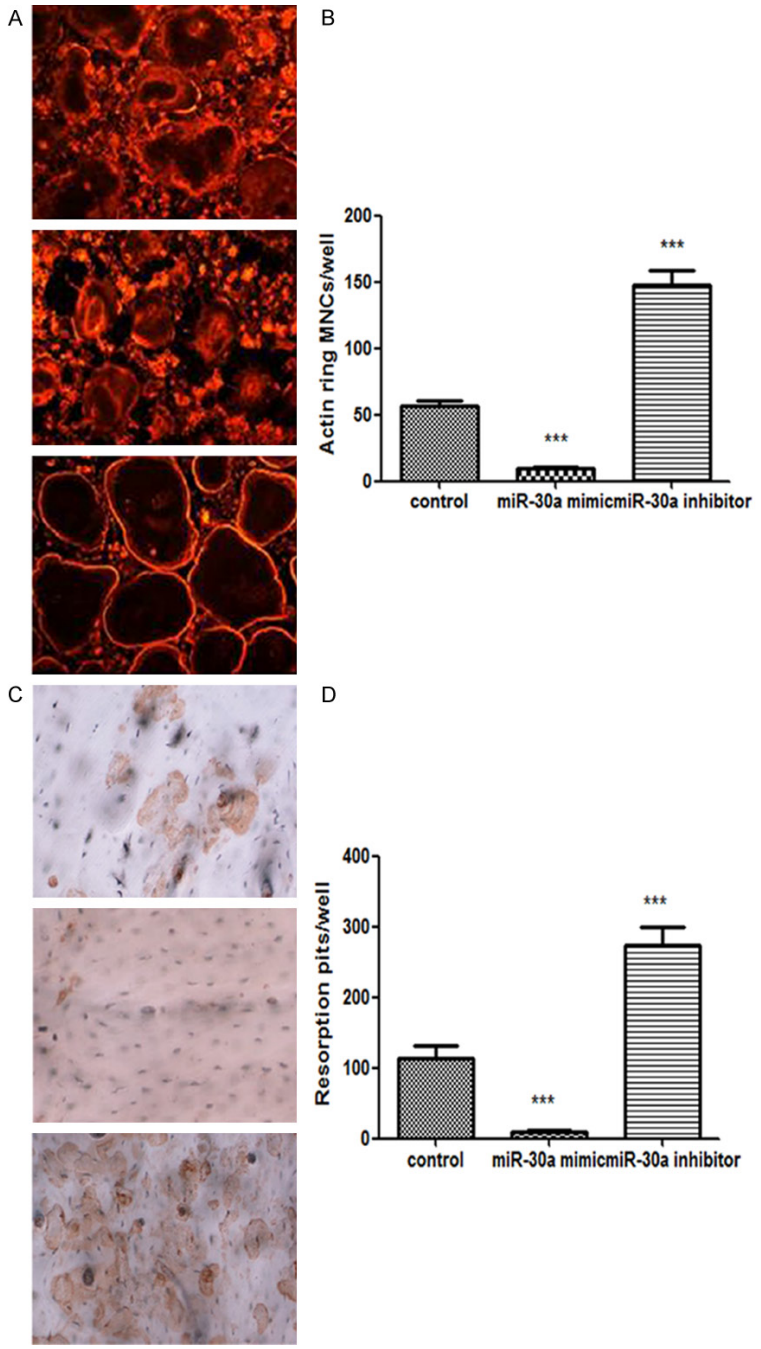

Figure 3. miR-30a attenuates actin ring formation and bone resorption. (A, B) BMMs were cultured for 2 days in the presence of M-CSF and RANKL. Two-day-old OCPs were transfected with a miR-30a mimic, miR-30a inhibitor, or negative control as indicated. Transfected cells were further cultured in the presence of M-CSF and RANKL. (A) Cells were fixed and stained with phalloidin. (B) Numbers of MNCs containing an actin ring were counted. Data represent means ± SD of triplicate samples. ***$p < 0.001$ vs. control. Results are representative of at least three independent sets of similar experiments. (C, D) BMMs were cultured on Osteo Assay plates for 2 days in the presence of M-CSF and RANKL. Two-day old OCPs were transfected with a miR-30a mimic, miR-30a inhibitor, or negative control as indicated. Transfected cells were further cultured for 36 h in presence with M-CSF and RANKL. (C) Resorption lacunae were visualized by bright-field microscopy. (D) Numbers of resorption pits were counted. Data represent means ± SD of triplicate samples. ***$p < 0.001$ vs. control. Results are representative of at least three independent sets of similar experiments.

Statistical analysis

SPSS11.0 was used to analyze our data. Quantitative data was expressed as mean ± SD. Non-paired T test was used to analyzed data between groups. A $p < 0.05$ was considered as statistically significant

Results

MiR-30a is down-regulated in RANKL-caused osteoclastogenesis

To identify miRNA expressions in RANKL-induced osteoclastogenesis, miRNA microarray analysis was used for detection. We cultured BMMs in the presence of M-CSF without or with RANKL for 72 hours prior to analysis. A total of 617 mouse miRNAs were analyzed, showing that 20 miRNAs were down-regulated by RANKL stimulation (green color far right third of array in **Figure 1A**). Twenty-nine miRNAs were up-regulated by RANKL stimulation (red color far right third of array in **Figure 1A**). Among these miRNAs, miR-30a was robustly decreased (**Figure 1A** arrow). Afterwards, we performed qRT-PCR to detect the levels of miR-30a during osteoclast differentiation. In accordance with the results from miRNA microarray, the level of miR-30a was progressively decreased in the process of RANKL-caused osteoclastogenesis (**Figure 1B**).

MiR-30a regulates RANKL-induced osteoclastogenesis negatively

Then we studied the function of miR-30a in the formation of

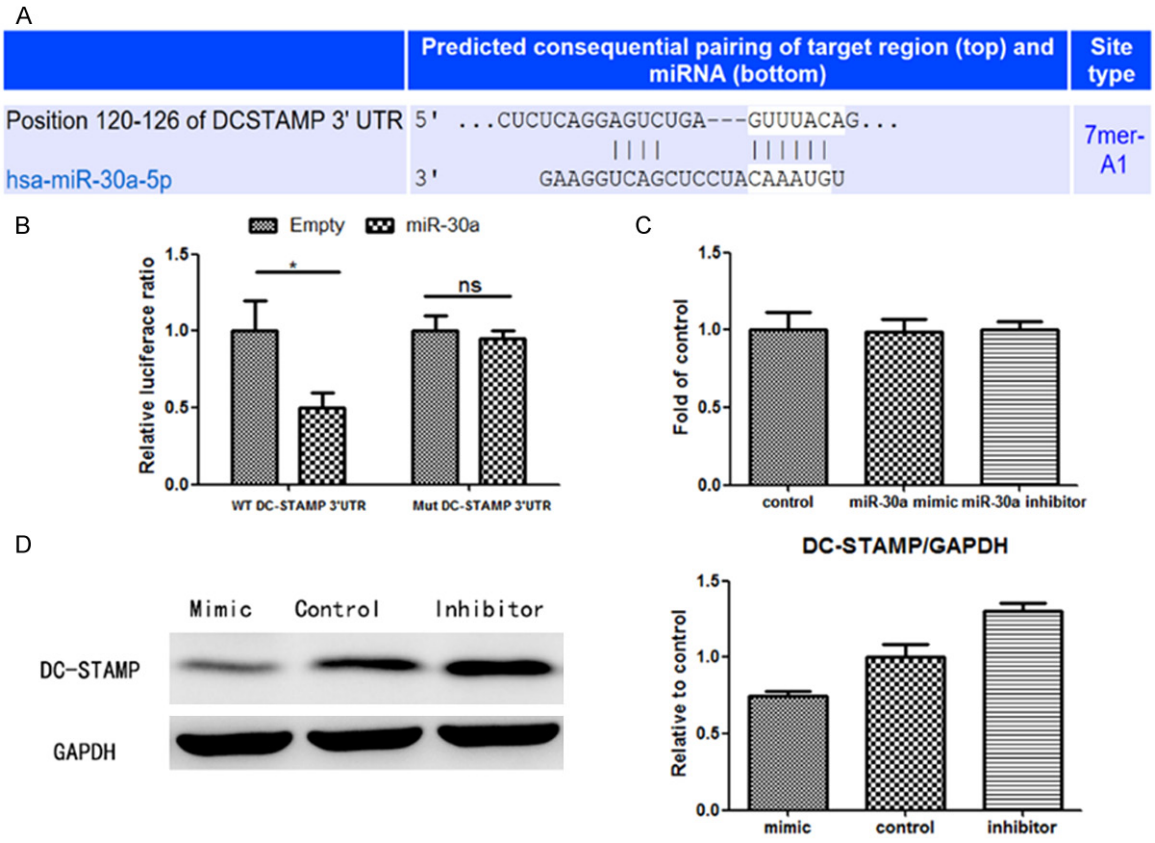

Figure 4. DC-STAMP is a direct target of miR-30a. (A) Biological prediction revealed that DC-STAMP could be a direct target of miR-30a. (B) Luciferase reporter assays in OCPs, with co-transfection of WT or Mut DC-STAMP and miR-30a as indicated. Transfection of miR-30a mimics markedly weakened luciferase activity of WT-DC-STAMP 3'-UTR. *$p < 0.05$. (C) Inhibition or overexpression of miR-30a in OCPs did not alter DC-STAMP mRNA level. (D) Overexpression of miR-30a significantly inhibited DC-STAMP protein expression.

osteoclasts. We found that miR-30a was down-regulated in advanced stage. Instead of focusing BMMs, we detected the influences of miR-30a on OCPs. We performed qRT-PCR analysis to confirm miR-30a mimics expression after OCPs were transfected (**Figure 2A**). As a result, the osteoclast formation induced by RANKL was obviously attenuated (**Figure 2B** and **2C**). To further verify our hypothesis, a miR-30a inhibitor was further transfected to detect the effect of miR-30a on osteoclastogenesis. Our data manifested the miR-30a inhibitor transfection successfully down-regulated miR-30a (**Figure 2D**). Moreover, as showed in **Figure 2E** and **2F**, the miR-30a inhibitor could significantly promote osteoclast formation. These results suggested that miR-30a was a negative regulator for RANKL-caused osteoclastogenesis.

The role of miR-30a on osteoclast function

Deeply, we explored the effect of miR-30a on osteoclast function. After OCPs were transfected with miR-30 mimics or inhibitors, they were stained with phallidin to determine the formation of actin ring. Interestingly, miR-30 mimics dramatically inhibited the formation of actin ring while the inhibitors promoted the formation compared with the control group (**Figure 3A** and **3B**). After that, pit formation test was performed to investigate the role of miR-30a in bone resorption activity. After transfection, the miR-30a mimics obviously inhibited the formation of resorption pit while the miR-30a inhibitors increased it (**Figure 3C** and **3D**). Therefore, results from our research revealed that miR-30a attenuated the formation and function of osteoclast during RANKL-induced osteoclasts formation.

MiR-30a inhibited osteoclastogenesis by directly targeting the 3'UTR of DC-STAMP

In order to investigate the potential molecular mechanism of miR-30a in regulating RANKL-induced formation of osteoclasts, we used Tar-

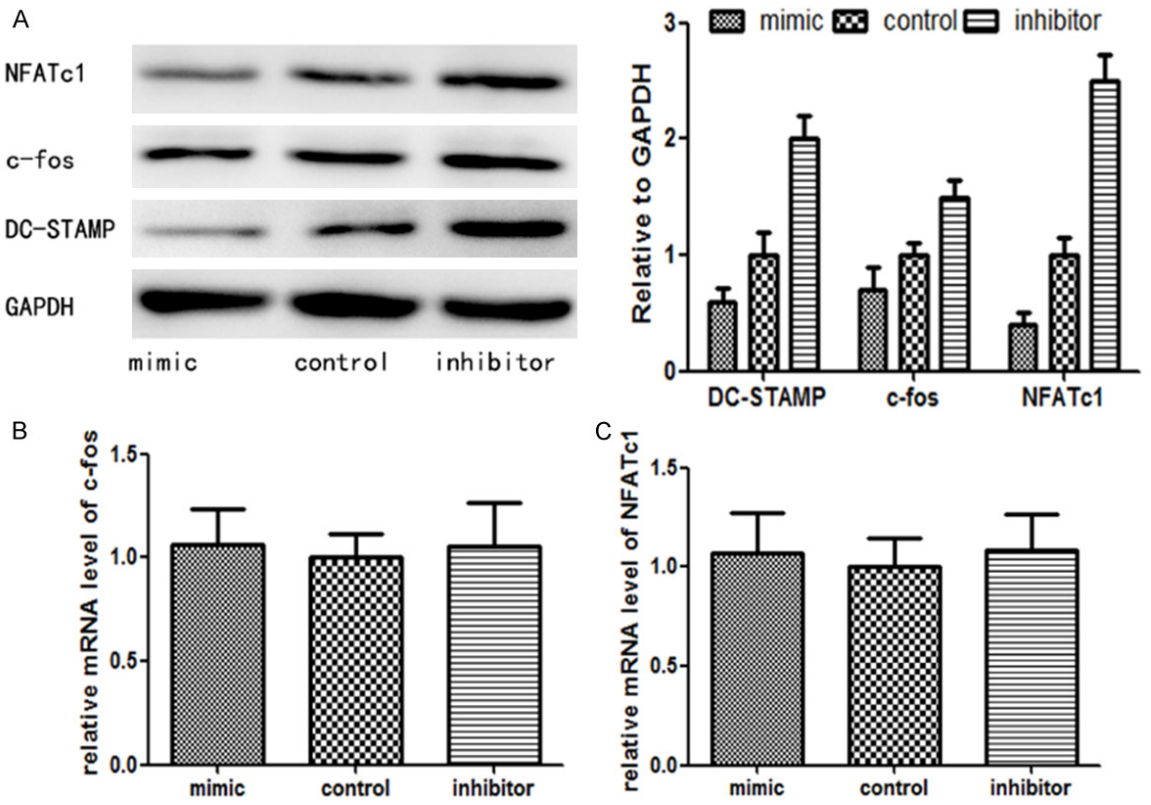

Figure 5. Overexpression of miR-30a suppressed DC-STAMP-c-fos-NFATc1 signaling pathway. BMMs were cultured for 2 days in the presence of M-CSF and RANKL. Two-day-old OCPs were transfected with a miR-30a mimic, miR-30a inhibitor, or negative control as indicated. (A) The effect of miR-30a on protein expression of DC-STAMP, c-fos and NFATc1, GAPDH was an internal reference. (B, C) The effect of miR-30a on the mRNA levels of c-Fos (B) and NFATc1 (C), analyzed by qRT-PCR. Results are representative of at least three independent sets of similar experiments.

getScan release 6.2 as wells as miR and a to search the target genes with an established function of stimulating osteoclastogenesis. Afterwards, we had the prediction that DC-STAMP could be a direct target of miR-30a. In the two databases, MiR-30a was predicted as highly conserved. We constructed luciferase reporter plasmids of wild type which contained the complete 3'UTR of DC-STAMP and muted type which contained a muted binding site at the 3'UTR to verify that prediction. Firstly, OCPs were transfected with a miR-30a mimic. We co-transfected the wild group and muted group with WT DC-STAMP plasmid and MT DC-STAMP plasmid, respectively. As a result, the normalized luciferase activity obviously declined in the WT cells and with the miR-30a mimic ($P < 0.05$). However, we did not detect any significant difference in MT plasmid group. Furthermore, we performed qRT-PCR as well as western blotting to validate the effect of miR-30a on the expression of DC-STAMP (**Figure 4C** and **4D**). Obviously, we concluded that protein expression of DC-STAMP was dramatically attenuated in the OCPs with the miR-30a mimic but upregulated with the transfection of a miR-30a inhibitor, while no changes were seen in the mRNA level of DC-STAMP.

MiR-30a inhibited RANKL-caused activation of DC-STAMP-c-Fos-NFATc1 signaling

To further investigate the underlying mechanisms of DC-STAMP-regulated osteoclasts formation, we detected the expression status of genes related to osteogenesis. It was reported that c-Fos-NFATc1 signaling took part in the formation of osteoclasts and bone resorption (12), so we measured the protein and mRNA levels of NFATc1 and c-fos. OCPs were transfected with miR-30a mimics or inhibitors and induced with 50 ng/ml RANKL and 50 ng/ml M-CSF for 72 hours. As a result, the protein level of DC-STAMP was obviously inhibited (**Figure 5A**). Consistently, with the upregulation of miR-30a, c-Fos and NFATc1 protein levels

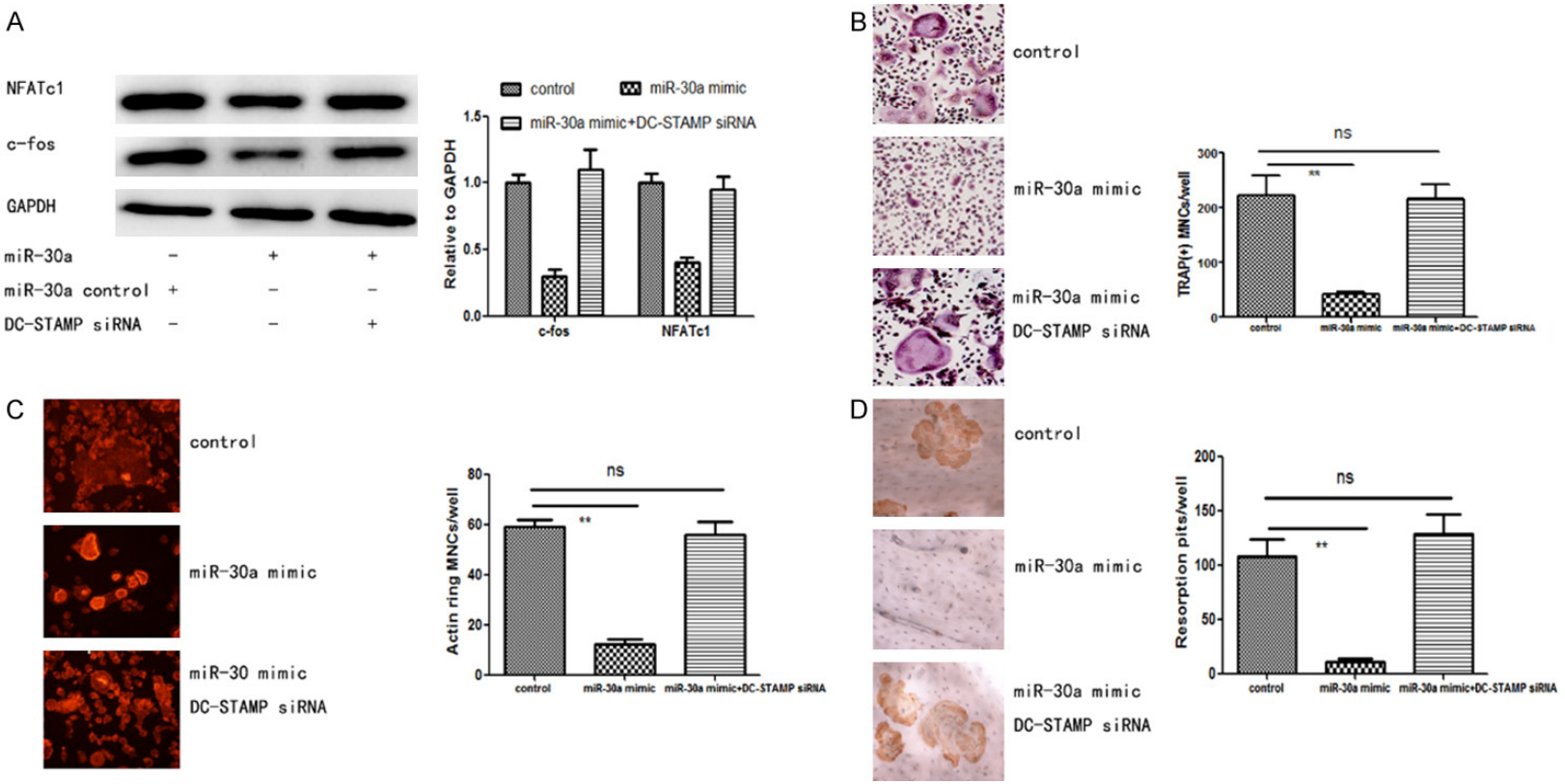

Figure 6. DC-STAMP was the target gene responsible for miR-30a triggered inhibition on osteoclastogenesis and bone resorption. BMMs were cultured for 2 days in the presence of M-CSF and RANKL. Two-day-old OCPs were pretransfected with DC-STAMP siRNA, followed by the transfection with miR-30a mimic. The effect of DC-STAMP siRNA on miR-30a inhibited expression of c-Fos and NFATc1 were analyzed by western blotting (A). The corresponding role on the number of TRAP + MNCs (B), actin ring formation (C) and bone resorption (D) were also examined. **P < 0.01. Results are representative of at least three independent sets of similar experiments.

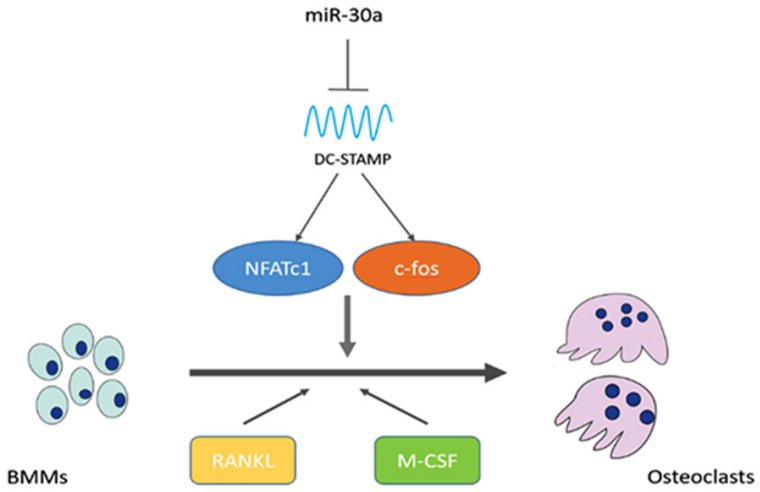

Figure 7. Illustration for miR-30a-mediated suppression of osteoclastogenesis. MiR-30a suppressed DC-STAMP expression leading to the inhibition of c-fos and NFATc1 in BMMs, thus inhibiting the effects of RANKL/M-CSF-induced osteoclastogenic differentiation from BMMs to multinucleated giant osteoclasts and bone resorption.

were also decreased (**Figure 5A**). However, the relative mRNA levels of c-Fos (**Figure 5B**) and NFATc1 (**Figure 5C**) had no significant changes compared to control. Next, we silenced DC-STAMP with a siRNA to further study whether miR-30a could inhibit the formation and function of osteoclasts. Following pre-transfection with DC-STAMP siRNA, we did not detect the inhibition effect of miR-30a on the expression of c-Fos and NFATc1 (**Figure 6A**). Other assays confirmed that DC-STAMP siRNA pretreatment obviously ameliorated the decline in the amount of mature osteoclasts induced by miR-30a up-expression (**Figure 6B**). Also, we did not detect any obvious differences for the inhibition effects of miR-30a on the formation of actin ring after cells were transfected with DC-STAMP siRNA (**Figure 6C**). At the same time, the bone resorption activity of mature osteoclasts also was promoted (**Figure 6D**). Taken together, our results validated that miR-30a inhibited the formation and function of osteoclasts via suppressing DC-STAMP-c-Fos-NFATc1 signaling.

Discussion

Both osteoclasts and osteoblasts are reported to regulate physical bone remodeling [14]. Pathologically speaking, the excessive activated osteoclasts activity often induce loss of bone mass which is the main cause of many bone disorders including osteoporosis [15]. As a common and progressive bone disorder, osteoporosis has a high risk of fracture. More and more people are diagnosed with osteoporosis with the increase of elder people [16, 17].

It was reported that various genes including NFATc1, NF-κB and c-Fos mediated RANKL-induced osteoclastogenesis [18] and costimulatory signals containing FcRγ and DAP12 are required. In addition, RANKL regulated negative regulators such as Bcl-6, MafB and IRF-8 to potentiate osteoclastogenesis [19-21]. Besides, RANKL mediated the formation of osteoclasts not only in the process of transcription but also post-transcription and post-translation [21, 22]. We proposed that miRNAs could regulate gene expression of osteoclasts differentiation as they could modulate differentiation of other cells. To find a new modulatory mechanism, we performed miRNA array to get the expression profiles and explored the effects of miR-30a in the process of osteoclastogenesis. This is the first evidence to verify miR-30a could modulate formation and function of osteoclasts post-transcriptionally.

In this study, we showed the miRNA expression profile during the formation of osteoclasts induced by RANKL. According to the results of microarray analysis, we found that miR-30a was down-regulated extremely among a series of miRNAs. Furthermore, we found that miR-30a negatively regulated RANKL-mediated osteoclastogenesis, as well as osteoclast function. Moreover, our study confirmed miR-30a straightly targeted DC-STAMP and inhibited its expression.

From it was discovered at the first time [23], DC-STAMP was recognized as a crucial molecule in modulating OCPs fusion as well as the differentiation of osteoclastogenesis [24]. Originally, DC-STAMP was detected and situated on dendritic cells [25]. Later, osteoclasts were also found expressing DC-STAMP [26].

Researchers found slight and severe osteoporotic symptoms in DC-STAMP-knock-out mice [27] and transgenic mice [28]. However, the underlying mechanisms remains unclear.

To further investigate the underlying mechanisms of DC-STAMP-regulated formation of osteoclasts, we detected the expression of genes related to osteogenesis. We measured the expression status of NFATc1 as well as c-fos on the mRNA and protein levels. Results showed that the levels of NFATc1 and c-Fos proteins were markedly suppressed following the transfection of miR-30a mimic consistent with the down-regulated proteins expression of DC-STAMP. However, this decreasing phenomena was not seen in the mRNA levels of NFATc1 and c-fos. We concluded from the above data that miR-30a modulated c-fos-NFATc1 signaling pathway via targeting DC-STAMP. To explore further whether miR-30a suppress the formation and function of osteoclasts, we used siRNA of DC-STAMP. After pretransfection with DC-STAMP siRNA, the inhibiting influence of miR-30a on the relative expression status of NFATc1 and c-Fos was abrogated. In addition, DC-STAMP siRNA pretreatment obviously ameliorated the decline in the amount of mature osteoclasts induced by miR-30a up-expression. Also, we did not detect the miR-30a inhibition effect on the formation of actin ring after transfecting cells with a DC-STAMP siRNA. At the same time, the bone resorption activity of mature osteoclasts also was promoted. Taken together, our results validated that miR-30a inhibited the formation and function of osteoclasts via suppressing DC-STAMP-c-Fos-NFATc1 signaling (**Figure 7**).

Altogether, results from our study verified that miR-30a modulated osteoclastogenesis directly by targeting DC-STAMP. Moreover, the c-Fos and NFATc1 expression decreased with suppressed DC-STAMP induced by miR-30a. As a results, we demonstrated that miRNA played a vital effect during the formation of osteoclasts. In the future, inhibiting osteoclasts formation via miRNA may be a new promising treatment for the management of osteoporosis and other osteoclast-related bone diseases.

Disclosure of conflict of interest

None.

Address correspondence to: Dr. Xiaobo Lu, The Orthopaedic Department, The Affliated Hospital of Southwest Medical University, Luzhou City, Sichuan Province, China. E-mail: cg2420004@163.com

References

[1] Boyle WJ, Simonet WS and Lacey DL. Osteoclast differentiation and activation. Nature 2003; 423: 337-342.

[2] Zhao R. Immune regulation of osteoclast function in postmenopausal osteoporosis: a critical interdisciplinary perspective. Int J Med Sci 2012; 9: 825-832.

[3] Collins FL, Williams JO, Bloom AC, Singh RK, Jordan L, Stone MD, McCabe LR, Wang EC and Williams AS. CCL3 and MMP-9 are induced by TL1A during death receptor 3 (TNFRSF25)-dependent osteoclast function and systemic bone loss. Bone 2017; 97: 94-104.

[4] Roodman GD. Cell biology of the osteoclast. Exp Hematol 1999; 27: 1229-1241.

[5] Lee J, Youn BU, Kim K, Kim JH, Lee DH, Seong S, Kim I, Han SH, Che X, Choi JY, Park YW, Kook H, Kim KK, Lim DS and Kim N. Mst2 controls bone homeostasis by regulating osteoclast and osteoblast differentiation. J Bone Miner Res 2015; 30: 1597-1607.

[6] Amend SR, Uluckan O, Hurchla M, Leib D, Novack DV, Silva M, Frazier W and Weilbaecher KN. Thrombospondin-1 regulates bone homeostasis through effects on bone matrix integrity and nitric oxide signaling in osteoclasts. J Bone Miner Res 2015; 30: 106-115.

[7] Gennari L, Bianciardi S and Merlotti D. MicroRNAs in bone diseases. Osteoporos Int 2017; 28: 1191-1213.

[8] Ambros V. The functions of animal microRNAs. Nature 2004; 431: 350-355.

[9] Bartel DP. MicroRNAs: genomics, biogenesis, mechanism, and function. Cell 2004; 116: 281-297.

[10] van Wijnen AJ, van de Peppel J, van Leeuwen JP, Lian JB, Stein GS, Westendorf JJ, Oursler MJ, Im HJ, Taipaleenmaki H, Hesse E, Riester S and Kakar S. MicroRNA functions in osteogenesis and dysfunctions in osteoporosis. Curr Osteoporos Rep 2013; 11: 72-82.

[11] Tang P, Xiong Q, Ge W and Zhang L. The role of microRNAs in osteoclasts and osteoporosis. RNA Biol 2014; 11: 1355-1363.

[12] Liu J, Dang L, Li D, Liang C, He X, Wu H, Qian A, Yang Z, Au DW, Chiang MW, Zhang BT, Han Q, Yue KK, Zhang H, Lv C, Pan X, Xu J, Bian Z, Shang P, Tan W, Liang Z, Guo B, Lu A and Zhang G. A delivery system specifically approaching bone resorption surfaces to facilitate therapeutic modulation of microRNAs in osteoclasts. Biomaterials 2015; 52: 148-160.

[13] Youn BU, Kim K, Kim JH, Lee J, Moon JB, Kim I, Park YW and Kim N. SLAT negatively regulates RANKL-induced osteoclast differentiation. Mol Cells 2013; 36: 252-257.
[14] Henriksen K, Karsdal MA and Martin TJ. Osteoclast-derived coupling factors in bone remodeling. Calcif Tissue Int 2014; 94: 88-97.
[15] Kang IS and Kim C. NADPH oxidase gp91phox contributes to RANKL-induced osteoclast differentiation by upregulating NFATc1. Sci Rep 2016; 6: 38014.
[16] Mattia C, Coluzzi F, Celidonio L and Vellucci R. Bone pain mechanism in osteoporosis: a narrative review. Clin Cases Miner Bone Metab 2016; 13: 97-100.
[17] Body JJ, Terpos E, Tombal B, Hadji P, Arif A, Young A, Aapro M and Coleman R. Bone health in the elderly cancer patient: a SIOG position paper. Cancer Treat Rev 2016; 51: 46-53.
[18] Asagiri M and Takayanagi H. The molecular understanding of osteoclast differentiation. Bone 2007; 40: 251-264.
[19] Zhao B, Takami M, Yamada A, Wang X, Koga T, Hu X, Tamura T, Ozato K, Choi Y, Ivashkiv LB, Takayanagi H and Kamijo R. Interferon regulatory factor-8 regulates bone metabolism by suppressing osteoclastogenesis. Nat Med 2009; 15: 1066-1071.
[20] Miyauchi Y, Ninomiya K, Miyamoto H, Sakamoto A, Iwasaki R, Hoshi H, Miyamoto K, Hao W, Yoshida S, Morioka H, Chiba K, Kato S, Tokuhisa T, Saitou M, Toyama Y, Suda T and Miyamoto T. The Blimp1-Bcl6 axis is critical to regulate osteoclast differentiation and bone homeostasis. J Exp Med 2010; 207: 751-762.
[21] Kim K, Kim JH, Lee J, Jin HM, Kook H, Kim KK, Lee SY and Kim N. MafB negatively regulates RANKL-mediated osteoclast differentiation. Blood 2007; 109: 3253-3259.
[22] Lee Y, Kim HJ, Park CK, Kim YG, Lee HJ, Kim JY and Kim HH. MicroRNA-124 regulates osteoclast differentiation. Bone 2013; 56: 383-389.
[23] Kukita T, Wada N, Kukita A, Kakimoto T, Sandra F, Toh K, Nagata K, Iijima T, Horiuchi M, Matsusaki H, Hieshima K, Yoshie O and Nomiyama H. RANKL-induced DC-STAMP is essential for osteoclastogenesis. J Exp Med 2004; 200: 941-946.
[24] Vignery A. Macrophage fusion: the making of osteoclasts and giant cells. J Exp Med 2005; 202: 337-340.
[25] Hartgers FC, Looman MW, van der Woning B, Merkx GF, Figdor CG and Adema GJ. Genomic organization, chromosomal localization, and 5' upstream region of the human DC-STAMP gene. Immunogenetics 2001; 53: 145-149.
[26] Rho J, Altmann CR, Socci ND, Merkov L, Kim N, So H, Lee O, Takami M, Brivanlou AH and Choi Y. Gene expression profiling of osteoclast differentiation by combined suppression subtractive hybridization (SSH) and cDNA microarray analysis. DNA Cell Biol 2002; 21: 541-549.
[27] Yagi M, Miyamoto T, Sawatani Y, Iwamoto K, Hosogane N, Fujita N, Morita K, Ninomiya K, Suzuki T, Miyamoto K, Oike Y, Takeya M, Toyama Y and Suda T. DC-STAMP is essential for cell-cell fusion in osteoclasts and foreign body giant cells. J Exp Med 2005; 202: 345-351.
[28] Iwasaki R, Ninomiya K, Miyamoto K, Suzuki T, Sato Y, Kawana H, Nakagawa T, Suda T and Miyamoto T. Cell fusion in osteoclasts plays a critical role in controlling bone mass and osteoblastic activity. Biochem Biophys Res Commun 2008; 377: 899-904.